

# Modeling the Interference of Pulsed Radar Signals in OFDM-Based Communications Systems

Ahmad Salim, Daniela Tuninetti, Natasha Devroye, Danilo Erricolo  
University of Illinois at Chicago, Chicago, IL 60607, USA  
Email: Ahmad.Salim@asu.edu, {danielat,devroye,derric1}@uic.edu

**Abstract**—Spectrum coexistence between radar and communications systems has received considerable attention recently as it has presented itself as one solution to the increasing demand for higher data rates in communications systems. This paper aims to model the interfering radar signal at the receiver of a communications system that uses orthogonal frequency-division multiplexing (OFDM). As an example, a rectangular-shaped pulsed radar signal is considered, for which the probability mass functions (PMFs) are derived for the amplitude and phase of the radar interference. The derived PMFs are shown to accurately model the radar interference generated via Monte Carlo simulations.

## I. INTRODUCTION

The increasing demand for wireless services and shortage of new spectral resources has motivated proposals calling for spectral coexistence between systems that are conventionally operated over independent bands. Consequently, a number of research institutes started pushing research inline with this vision. For instance, the National Science Foundation (NSF) initiated the “enhancing access to the radio spectrum” program, known as EARS [1], and the Defense Advanced Research Projects Agency (DARPA) started the “shared spectrum access for radar and communications” program [2]. DARPA has also initiated a series of competitive matches called the Spectrum Collaboration Challenge (SC2) in which teams compete in developing intelligent radio networks capable of optimizing the usage of the radio frequency (RF) spectrum according to the varying RF environment. The goal is to determine when, where and how to distribute (or share) the spectrum resources among different radio networks. One of the candidate bands for spectrum sharing is the S-band (2-4 GHz), which is currently used by several radar systems (e.g., air traffic control, Navy surveillance, and weather), and where wireless communication systems (e.g., WiFi and WLAN) operate. This problem can be looked at from different angles, for instance, one can study how can either communications or radar systems be changed such that they can efficiently coexist with each other. Another interesting direction is the joint design of these systems to share the spectrum. Herein, we are specifically interested in investigating the impact of unaltered radar systems on communications systems as a starting point for practical code design to mitigate this impact.

There have been experimental studies on spectrum coexistence between conventional (unchanged) radar and communication systems. NTIA studies in [3] concluded that radars are sensitive to the effects of interference from communications systems. Interestingly, [3] also show that radars are robust against interference from other radars.

In a related line of research, there have been numerical as well as practical studies to quantify the effect of radar interference over communications systems. For instance, [4] simulates the effect of swept radars interference on the performance of a WiMAX system, and shows that reliable spectrum coexistence can be achieved via cooperative sensing algorithms. In [5], an LTE packet scheduling algorithm mitigates the radar interference by discarding users that are severely affected by the radar interference.

Refs. [6–8], experimentally study the performance degradation that can occur on both sides of coexisting air traffic control radar and LTE systems in the S-band. Regarding the effect on LTE systems, [6–8] report that a significant degradation in performance takes place in the TDD bands when the radar pulses hit the packets intended for synchronization. Among the possible mitigation techniques, improved filtering and spectrum sensing for both systems were discussed.

In our previous research [9–11], we have analytically studied the effect of radar interference on the performance of a single-carrier communications system over an additive white Gaussian noise (AWGN) channel. Therein, we modelled the radar signal as additive interference of deterministic amplitude (that can be estimated at the receiver of the communications system) and an unknown random phase uniformly distributed in  $[0, 2\pi]$ . In this paper, we consider an OFDM-based multi-carrier communications system, and model the additive radar interference after being processed by a conventional OFDM receiver. Specifically, we derive the PMFs of the amplitude and phase of that interference.

Even though the adopted model in [9–11] is a good approximation in general, the literature lacks an accurate theoretical model of pulsed radar interference from the perspective of an OFDM receiver. This paper models the interference of rectangular-shaped pulsed radar under a number of assumptions. In our study, we assume that all the parameters of the periodic radar signal are known (or can be estimated) except its propagation delay, which results in the assumption that the time shift between the signals of the two systems is random. The major findings regarding the radar interference include:

- The amplitude and the phase of the radar signal are correlated random variables, and their marginal PMFs as well as their joint one can be accurately estimated in a numerical manner given the knowledge of some of the parameters of the radar signal.
- For a rectangular pulsed radar signal, the following points were concluded:

- The joint PMF as well as the marginal ones of the amplitude and the phase can be further expressed in closed forms. In this case, we found that the amplitude changes across subcarriers but remains constant between different symbols over the same subcarrier index. On the other hand, the phase changes across both symbols and subcarriers.
- The marginal PMF of the amplitude consists of a mixture of a small number of delta functions (whose number depends on the width of the radar pulse), and one mass point dominates the probability. The dominant mass point depends on the subcarrier index  $k$ , and hence the amplitude can be approximated by a deterministic function of  $k$ .
- The marginal PMF of the phase is a weighted combination of  $N_A$  discrete uniform PMFs where  $N_A$  is the number of distinct amplitudes of the post-processed radar signal.
- The joint PMF is composed of a weighted sum of multiple discrete uniform PMFs; each one corresponds to a specific amplitude value.
- The derived PMFs are shown to accurately model the radar interference generated via Monte Carlo simulations under a number of simplifying assumptions.

Notation: Table I summarizes some of the most frequently used symbols and operators in this paper.

TABLE I: Notation and symbols.

$C$ (as a subscript)	Communications system parameter.
$R$ (as a subscript)	Radar system parameter.
$[a, b, n]$	Finite arithmetic sequence with $n$ terms with $a$ and $b$ as the initial and final terms, respectively, i.e., $[a, b, n] = \{x x = a + ri, r = (b - a)/(n - 1), i \in [0 : n - 1]\}$ .
$\mathcal{U}\{\mathcal{S}\}$	Discrete uniform distribution over elements of the set $\mathcal{S}$ .
$\mathcal{U}\{a, b, n\}$	Discrete uniform distribution over $[a, b, n]$ .
$(a)_N$	$a$ modulo $N$ .
$\{\mathcal{S}\}_c$	$\{\mathcal{S}\}_c = \begin{cases} \mathcal{S}, & c \text{ is true} \\ \emptyset, & \text{else} \end{cases}$
$ \cdot $	Magnitude of a complex number or cardinality of a set.

## II. COEXISTENCE MODEL

The signal of the OFDM-based communications system consists of  $M$  OFDM symbols wherein each OFDM symbol spans  $T_C$  seconds. Furthermore, it operates at a carrier frequency of  $f_C$  Hz with  $N$  subcarriers over a total bandwidth of  $B_C$  Hz. The number of samples used for the cyclic prefix is given by  $N_{CP}$ . The considered radar system is a pulsed radar system that operates at a carrier frequency  $f_R$  Hz with a pulse width of  $\tau_R$  seconds. The pulse repetition interval (PRI) of the passband radar signal  $w_R(t)$  is given by  $T_R$ . We assume that, when received at the communications system, the received radar signal lags that of the communications system by  $t_d$  seconds.

## III. RADAR INTERFERENCE AT THE OUTPUT OF AN OFDM RECEIVER

Assuming the knowledge of the time instants at which the OFDM symbols start, the communications system receiver can sample in synchrony with the transmitted symbols at the instants  $t = nT_S$ ,  $n \in \mathbb{Z}^*$ , where  $T_S = 1/B_C$  is the sampling

period in seconds. After sampling, removing the cyclic prefix of length  $N_{CP}$ , and performing an  $N$ -point discrete Fourier transform (DFT), the part of the received signal corresponding to the radar interference on the  $k$ th subcarrier during the  $m$ th block can be written as

$$I_{k,m} = \frac{1}{\sqrt{N}} \sum_{n=mN_C+N_{CP}}^{mN_C+N+N_{CP}-1} w_R(nT_S - n_d T_S) \times e^{j2\pi f_R(nT_S - n_d T_S)} e^{-j2\pi f_C(nT_S)} e^{-j2\pi k \frac{(n-mN_C-N_{CP})}{N}} \quad (1)$$

where  $n_d = \lfloor \frac{t_d}{T_S} \rfloor$ ,  $N_C = \lceil \frac{T_C}{T_S} \rceil$  and  $N_R = \lceil \frac{T_R}{T_S} \rceil$ . The reader should note that the modeling of the up-conversion of the radar signal to its carrier band and the down-conversion at the OFDM receiver does not reflect the exact implementation in a practical system; however, it simplifies the derivations while capturing the effect of having different carrier frequencies for the radar and communications systems. By letting  $u = n - mN_C - N_{CP}$ ,  $I_{k,m}$  can be rewritten as

$$\begin{aligned} I_{k,m} &= \frac{1}{\sqrt{N}} \sum_{u=0}^{N-1} w_R(T_S(u + mN_C + N_{CP} - n_d)) \times \\ &\quad e^{j2\pi f_R T_S(u + mN_C + N_{CP} - n_d)} e^{-j2\pi f_C T_S(u + mN_C + N_{CP})} e^{-j2\pi k \frac{u}{N}} \\ &= \frac{1}{\sqrt{N}} \sum_{u=0}^{N-1} [v_{R,m}[u] e^{j2\pi \Delta T_S u} e^{-j2\pi k \frac{u}{N}}] e^{j\psi_m} \\ &= \text{DFT} \left( v_{R,m}[u] e^{j2\pi u \Delta T_S} \right) e^{j\psi_m} \end{aligned} \quad (2)$$

where  $v_{R,m}[u] = w_R((u + mN_C + N_{CP} - n_d) T_S)$ ,  $u \in [0 : N - 1]$ , is the sampled version of  $w_R(\cdot)$  during the  $m$ th OFDM block,  $\Delta = f_R - f_C$ , and  $\psi_m = 2\pi \Delta T_S (mN_C + N_{CP}) - 2\pi f_R T_S n_d$ .

Note that using the discrete-time representation in (1)–(2) coupled with the assumption that  $\tau_R \leq T_C \leq T_R$ , there will possibly exist OFDM blocks that do not experience any radar interference.

## IV. EXAMPLE: RECTANGULAR RADAR PULSE

In this case, the discrete-time radar signal corresponding to the  $m$ th block of length  $N$  (after removing the cyclic prefix at the OFDM receiver) is given by a rectangular signal, i.e., its sampled version and its corresponding DFT are respectively given by

$$v_{R,m}[n] = \begin{cases} A_R, & c_m \leq n \leq d_m - 1 \\ 0, & \text{else} \end{cases}, \quad n \in [0 : N - 1], \quad (3)$$

and

$$\begin{aligned} V_{R,m}[k] &= \text{DFT}(v_{R,m}[n]) \\ &= \begin{cases} \frac{A_R}{\sqrt{N}} (d_m - c_m), & k = 0 \\ \frac{A_R}{\sqrt{N}} e^{-j\pi(d_m + c_m - 1) \frac{k}{N}} \frac{\sin(\pi k (d_m - c_m)/N)}{\sin(\pi k/N)}, & k \in [1 : N - 1] \end{cases} \end{aligned} \quad (4)$$

where  $c_m$  and  $d_m$  are the beginning and end of the non-zero content of  $v_{R,m}[n]$ , and  $A_R \geq 0$  is its amplitude. We make a number of assumptions in the remainder of the text that we refer to when applicable, including:

- A.1**  $\Delta N T_S$  is an integer number.
- A.2**  $T_R = T_C$ .
- A.3**  $T_R$ ,  $\tau_R$  and  $t_d$  are multiples of  $T_S$ .
- A.4**  $t_d$  is uniformly distributed on  $[0, T_R - \tau_R]$ .

Substituting (4) in (2), we obtain

$$\begin{aligned} I_{k,m} &\stackrel{A.1}{=} V_{R,m} [(k - \Delta NT_S)_N] e^{j\Psi_m} \\ &= \begin{cases} \frac{A_R}{\sqrt{N}} (d_m - c_m) e^{j\Psi_m}, & k = \Delta NT_S \\ \frac{A_R}{\sqrt{N}} \cdot \frac{|\sin(\pi k_N (d_m - c_m)/N)|}{\sin(\pi k_N/N)} e^{j\Psi'_{k,m}}, & \text{else} \end{cases} \\ &= A_{k,m} e^{j\Phi_{k,m}} \end{aligned} \quad (5)$$

where  $A_{k,m}$  and  $\Phi_{k,m}$  are the amplitude and phase of  $I_{k,m}$ , respectively,  $k_N = (k - \Delta NT_S)_N$ ,  $\Psi'_{k,m} = \Psi_m + \pi\beta_{k,m} - \pi(d_m + c_m - 1) \frac{k_N}{N}$  and

$$\beta_{k,m} = \begin{cases} 0, & 0 \leq \left( \frac{k_N (d_m - c_m)}{N} \right)_2 \leq 1 \\ 1, & \text{else} \end{cases}.$$

To make the analysis tractable, we make the assumption in A.2. Let  $n_R = \lfloor \frac{\tau_R + l_d}{T_S} \rfloor$ . If  $n_R \leq N_{CP}$ , then  $v_{R,m}[n] = 0 \forall n \in [0 : N - 1]$  and  $m \in [0 : M - 1]$ . Otherwise,  $v_{R,m}[n]$  is given by (3) with  $d_m = n_R - N_{CP}$  and

$$c_m = \begin{cases} n_d - N_{CP}, & n_d > N_{CP} \\ 0, & \text{else} \end{cases}.$$

In the sequel of this section, we find the joint and marginal PMFs of the amplitude and the phase of the radar interference signal for the two cases of  $I_{k,m}$  as in (5). Below, we further assume A.3, and hence  $n_d = \frac{l_d}{T_S}$ , and  $n_R = \frac{\tau_R + l_d}{T_S}$ . We also denote the radar pulse width in samples by  $n_w = \frac{\tau_R}{T_S}$ .

A. Case I:  $k \in [0 : N - 1] \setminus \{\Delta NT_S\}$

In this case,  $A_{k,m}$  and  $\Phi_{k,m}$ ,  $k \in [0 : N - 1] \setminus \{\Delta NT_S\}$  and  $m \in [0 : M - 1]$ , can be written as

$$(A_{k,m}, \Phi_{k,m}) = \begin{cases} (0, \theta^1), & n_d \in \mathcal{D}_{1,k} \\ (\alpha_{2,k}[n_d], a_{2,k}n_d + b_{2,k,m} + \pi\beta_{k,m}), & n_d \in \mathcal{D}_{2,k}, (6) \\ (\alpha_{3,k}, a_{3,k}n_d + b_{3,k,m} + \pi\beta_{k,m}), & n_d \in \mathcal{D}_{3,k} \end{cases}$$

where

$$\begin{aligned} \alpha_{2,k}[n] &= \frac{A_R}{\sqrt{N}} \cdot \frac{|\sin(\pi k_N (n + n_w - N_{CP})/N)|}{\sin(\pi k_N/N)}, \\ \alpha_{3,k} &= \frac{A_R}{\sqrt{N}} \cdot \frac{|\sin(\pi k_N (n_w)/N)|}{\sin(\pi k_N/N)}, \\ \mathcal{S}_{0,k} &= \{x | x \in [N_{CP} - n_w + 1 : N_{CP} - 1], \\ &\quad x = \frac{nN}{k_N} + N_{CP} - n_w, \frac{nN}{k_N} \in \mathbb{Z}^+, n \in \mathbb{Z}^+\}, \\ \mathcal{S}_{1,k} &= \{x | x \in [N_{CP} - n_w + 1 : N_{CP} - 1], \\ &\quad |\sin(\pi k_N (x + n_w - N_{CP})/N)| = |\sin(\pi k_N (n_w)/N)|\}, \\ N_{1,k} &= |\mathcal{S}_{0,k}| + |\mathcal{S}_{1,k}| - e_k N_{3,k} + N_R - 2n_w + 2, \\ N_{3,k} &= N_R - n_w - N_{CP} + |\mathcal{S}_{1,k}| + 1, \\ \mathcal{D}_{1,k} &= [0 : N_{CP} - n_w] \cup \mathcal{S}_{0,k} \cup \{[N_{CP} : N_R - n_w]\}_{n_w \in \mathcal{S}_{w,k}}, \\ \mathcal{D}_{2,k} &= [N_{CP} - n_w + 1 : N_{CP} - 1] \setminus \{\mathcal{S}_{0,k} \cup \mathcal{S}_{1,k}\}, \\ \mathcal{D}_{3,k} &= \{[N_{CP} : N_R - n_w] \cup \mathcal{S}_{1,k}\}_{n_w \notin \mathcal{S}_{w,k}}, \\ \mathcal{S}_{w,k} &= \left\{ nN/k_N \mid n \in \mathbb{Z}^+ \right\}, \\ a_{2,k} &= -2\pi f_R T_S - \pi \frac{k_N}{N}, \end{aligned}$$

<sup>1</sup>Even though  $\Phi_{k,m}$  is undefined whenever  $A_{k,m}$  is zero, for analytical tractability, we assume that it is given by  $\theta$  where  $\theta \sim \mathcal{U}\{0, 2\pi, N_{1,k}\}$ .

$$\begin{aligned} b_{2,k,m} &= 2\pi \Delta T_S (mN_C + N_{CP}) - \pi(n_w - N_{CP} - 1) \frac{k_N}{N}, \\ a_{3,k} &= -2\pi f_R T_S - 2\pi \frac{k_N}{N}, \\ b_{3,k,m} &= 2\pi \Delta T_S (mN_C + N_{CP}) - \pi(n_w - 2N_{CP} - 1) \frac{k_N}{N}, \end{aligned}$$

and  $e_k$  is an indicator function defined as

$$e_k = \begin{cases} 0, & \text{if } \exists n \text{ s.t. } n_w = \frac{nN}{k_N}, n \in \mathbb{Z}^+ \\ 1, & \text{else} \end{cases}.$$

The set  $\mathcal{S}_{0,k}$  consists of all values of  $n_d$  in  $[N_{CP} - n_w + 1 : N_{CP} - 1]$  such that  $A_k$  is zero in that range. From (6), we can draw the following conclusions:

- The amplitude changes across subcarriers but remains constant between different symbols over the same subcarrier index. Hence, we drop the block index  $m$  from  $A_{k,m}$  through the rest of paper.
- The phase changes across both symbols and subcarriers as a result of the difference in carrier frequencies of the two systems. In addition to the trivial  $\Delta = 0$  case, an exception arises when  $\Delta N_C T_S$  is an even number, wherein the phase changes across  $k$  but remains constant for different values of  $m$  over the same subcarrier.

Assuming A.4 holds, or equivalently  $n_d \sim \mathcal{U}\left\{0 : \frac{T_R - \tau_R}{T_S}\right\}$ , then we can express the PMFs of the amplitude and the phase of the radar interference signal based on the fact that both  $A_k$  and  $\Phi_{k,m}$  are transformations of the random variable (RV)  $n_d$ . Nonetheless, it should be noted that these transformation are non-monotonic in general, and hence the case where different values of the RV may correspond to the same transformed value. In such a case, the mass at that value of the RV is equal to the sum of probabilities of the different values leading to the same transformed value.

The marginal PMFs of the amplitude and phase of the radar signal over the  $k$ th subcarrier and during the  $m$ th OFDM symbol can be written respectively as

$$P_{A,k}[a] = \frac{N_{1,k}}{N_{Rw}} \delta[a] + \frac{1}{N_{Rw}} \sum_{n \in \mathcal{D}_{2,k}} \delta[a - \alpha_{2,k}[n]] + \frac{e_k N_{3,k}}{N_{Rw}} \delta[a - \alpha_{3,k}]$$

$$P_{\Phi,k,m}[\phi] = \frac{N_{1,k}}{N_{Rw}} \mathcal{Q}_{1,k}[\phi] + \frac{N_{2,k}}{N_{Rw}} \mathcal{Q}_{2,k,m}[\phi] + \frac{e_k N_{3,k}}{N_{Rw}} \mathcal{Q}_{3,k,m}[\phi]$$

where  $N_{Rw} = N_R - n_w + 1$ ,  $\delta[\cdot]$  is the Dirac delta function, and  $N_{2,k} = n_w - |\mathcal{S}_{0,k}| - |\mathcal{S}_{1,k}| - 1$ .  $\mathcal{Q}_{1,k}[\phi]$ ,  $\mathcal{Q}_{2,k,m}[\phi]$  and  $\mathcal{Q}_{3,k,m}[\phi]$  are the PMFs of the discrete uniform random variables characterized by  $\mathcal{U}\{0, 2\pi, N_{1,k}\}$ ,  $\mathcal{U}\{y | y = a_{2,k}n + b_{2,k,m}, n \in \mathcal{D}_{2,k}\}$  and  $\mathcal{U}\{y | y = a_{3,k}n + b_{3,k,m}, n \in \mathcal{D}_{3,k}\}$ , respectively.

Having written the amplitude and the phase in (6) over matching disjoint sets, the joint PMF can be easily written in terms of the conditional PMFs. Simply put, the phase of the interference given a specific amplitude is uniformly distributed. The joint PMF is given by

$$\begin{aligned} P_{A,\Phi,k,m}[a, \phi] &= \mathbb{P}[A_k = a, \Phi_{k,m} = \phi] \\ &= \mathbb{P}[\Phi_{k,m} = \phi | A_k = a] \times P_{A,k}[a] \\ &= \frac{1}{N_{Rw}} \left( P_{1,k}[a, \phi] + \sum_{\alpha \in \mathcal{X}_{2,k}} P_{2,\alpha,k,m}[a, \phi] + e_k P_{3,k,m}[a - \alpha_{3,k}, \phi] \right), \end{aligned} \quad (7)$$

where

$$\begin{aligned}
P_{1,k}[a, \phi] &= \sum_{\psi \in [0, 2\pi, N_{1,k}]} \delta[a, \phi - \psi], \\
P_{2,\alpha,k,m}[a, \phi] &= \sum_{\Psi \in \mathcal{Y}_{2,\alpha,k}} |\mathcal{Y}_{2,\alpha,\Psi,k}| \delta[a - \alpha, \phi - \Psi], \\
P_{3,k,m}[a, \phi] &= \sum_{\Psi \in \mathcal{Y}_{3,k}} |\mathcal{Y}_{3,\Psi,k}| \delta[a, \phi - \Psi], \\
\mathcal{Y}_{2,\alpha,k} &= \{y | y = a_{2,k}n + b_{2,k,m}, \alpha = \alpha_{2,k}[n], n \in \mathcal{D}_{2,k}\}, \\
\mathcal{X}_{2,k} &= \{x | x = \alpha_{2,k}[n], n \in \mathcal{D}_{2,k}\}, \\
\mathcal{Y}_{2,\alpha,\Psi,k} &= \{y | y = \Psi, y \in \mathcal{Y}_{2,\alpha,k}\}, \\
\mathcal{Y}_{3,k} &= \{y | y = a_{3,k}n + b_{3,k,m}, n \in \mathcal{D}_{3,k}\},
\end{aligned}$$

and  $\mathcal{Y}_{3,\Psi,k} = \{y | y = \Psi, y \in \mathcal{Y}_{3,k}\}$ .

We remark that the marginal PMF of the amplitude,  $P_{A,k}[a]$ , consists of a small number of delta functions ( $n_w + 2$  at most). Further, supported by numerical evaluations, we note that, in general, only one mass point dominates this PMF. The dominant mass point depends on the subcarrier index  $k$ . Hence, the amplitude can be approximated by a deterministic function of  $k$  as

$$\begin{aligned}
A_k &\approx \arg \max_{a \in \mathcal{S}_{A,k}} P_{A,k}[a] \\
&= \begin{cases} 0, & N_{1,k} > \max\{N_{2,x,k}, N_{3,k}\} \\ x_{2,k}, & N_{2,x,k} > \max\{N_{1,k}, N_{3,k}\} \\ \alpha_{3,k}, & N_{3,k} > \max\{N_{1,k}, N_{2,x,k}\} \end{cases} \quad (8)
\end{aligned}$$

where

$$\begin{aligned}
N_{2,x,k} &= \max_{n \in \mathcal{D}_{2,k}} \sum \delta[a - \alpha_{2,k}[n]], \\
x_{2,k} &= \arg \max_{n \in \mathcal{D}_{2,k}} \sum \delta[a - \alpha_{2,k}[n_d]],
\end{aligned}$$

and  $\mathcal{S}_{A,k}$  is the sample space of  $A_k$ . On the other hand, we note that the marginal PMF of the phase,  $P_{\Phi,k,m}[\phi]$ , is composed of unequally-weighted discrete uniform PMFs, namely,  $Q_{1,k}[\phi]$ ,  $Q_{2,k,m}[\phi]$  and  $Q_{3,k,m}[\phi]$ .

The model in [9–11] can be viewed as an approximation of the one derived herein, specifically, compared to our model, the PMF of the phase in [9–11] represents the conditional PMF of the phase given the dominant amplitude among all possible non-zero values. Moreover, the deterministic amplitude in [9–11] can be considered as the approximation in (8).

### B. Case II: $k = \Delta NT_S$

For this specific value of  $k$ , the amplitude and phase of  $I_{k,m}$  can be written as

$$(A_k, \Phi_{k,m}) = \begin{cases} (0, \theta), & n_d \in \mathcal{D}_1 \\ (\alpha_2[n_d], c \cdot n_d + b_m), & n_d \in \mathcal{D}_2, \\ (\alpha_3, c \cdot n_d + b_m), & n_d \in \mathcal{D}_3 \end{cases}$$

where

$$\begin{aligned}
\mathcal{D}_1 &= [0 : N_{CP} - n_w], \\
\mathcal{D}_2 &= [N_{CP} - n_w + 1 : N_{CP} - 1], \\
\mathcal{D}_3 &= [N_{CP} : N_R - n_w],
\end{aligned}$$

$$\theta \sim \mathcal{U}\{0, 2\pi, |\mathcal{D}_1|\},$$

$$\alpha_3 = \frac{A_R}{\sqrt{N}} n_w,$$

$$\alpha_2[n] = \frac{A_R}{\sqrt{N}} (n + n_w - N_{CP}),$$

$$b_m = 2\pi \Delta T_S (mN_C + N_{CP}),$$

and  $c = -2\pi f_R T_S$ .

The marginal PMFs of the amplitude and phase can be written respectively as

$$P_{A,k}[a] = \frac{N_{1,k}}{N_{Rw}} \delta[a] + \frac{1}{N_{Rw}} \sum_{n=N_{CP}-n_w+1}^{N_{CP}-1} \delta[a - \alpha_2[n]] + \frac{N_{3,k}}{N_{Rw}} \delta[a - \alpha_3],$$

and

$$P_{\Phi,k,m}[\phi] = \frac{N_{1,k}}{N_{Rw}} Q_{1,k}[\phi] + \frac{N_{2,k}}{N_{Rw}} Q_{2,k,m}[\phi] + \frac{N_{3,k}}{N_{Rw}} Q_{3,k,m}[\phi],$$

where  $N_{1,k} = N_{CP} - n_w + 1$ ,  $N_{2,k} = n_w - 1$ , and  $N_{3,k} = N_R - n_w - N_{CP} + 1$ . The PMFs  $Q_{1,k}[\phi]$ ,  $Q_{2,k,m}[\phi]$  and  $Q_{3,k,m}[\phi]$  are characterized by  $\mathcal{U}\{0, 2\pi, N_{1,k}\}$ ,  $\mathcal{U}\{\{y | y = c \cdot n + b_m, n \in \mathcal{D}_{2,k}\}\}$  and  $\mathcal{U}\{\{y | y = c \cdot n + b_m, n \in \mathcal{D}_{3,k}\}\}$ , respectively. The joint PMF is given by (7) with setting  $e_k = 1$ . Similar conclusions drawn for Case I about the PMFs apply for Case II. We skip discussing them for brevity.

## V. NUMERICAL EVALUATIONS

As an example, we consider an OFDM-based communications system operating at a carrier frequency of  $f_C = 2.84952$  GHz with  $N = 64$  subcarriers and total bandwidth of 960 kHz. The number of samples used for the cyclic prefix is  $N_{CP} = 16$  and  $M = 10$  blocks. The selection of the available bandwidth is consistent with, for example, an LTE communications system. The considered radar system is a pulsed radar system that operates at a carrier frequency  $f_R = 2.85$  GHz. To evaluate the derived PMFs, we consider a rectangular pulse with amplitude  $A_R = 2.5$  and width  $n_w = 4$  samples. With these parameters, the assumptions made in Section IV are all valid, and hence we can use the theoretical results obtained therein.

Fig. 1 shows some examples of the joint PMF of  $A_k$  and  $\Phi_{k,m}$  for various  $k$  values during the first OFDM block. We remark that the theoretical results closely match those from simulation in terms of both the values that  $A_k$  and  $\Phi_{k,m}$  take and the corresponding probabilities, which shows the validity of the theoretical findings. As shown in Fig. 1, the joint PMF is composed of a weighted sum of multiple uniform PMFs of  $\phi$ , where each one corresponds to a specific value of the amplitude that depends on the subcarrier index  $k$ . Furthermore, the number of mass points of the uniform functions is variable.

Due to the large number of mass points in the PMFs, we opted to only show theoretical results graphically. However, to quantify the accuracy of the theoretical findings we use the Jensen–Shannon divergence (JSD) to measure the distance between the simulated and the analytical joint PMFs. The JSD is a distance metric that is calculated using the Kullback–Leibler divergence (KLD) between two bivariate distributions ( $P$  and  $Q$ ) of the RVs  $A$  and  $\Phi$  as  $\text{JSD}(P||Q) = \frac{1}{2} \text{KLD}(P||M) + \frac{1}{2} \text{KLD}(Q||M)$  where  $M = \frac{1}{2}(P +$

$Q$ ) and  $\text{KLD}(P\|Q) = \sum_{\forall (a,\phi)} P(a,\phi) \log \frac{P(a,\phi)}{Q(a,\phi)}$ . For the dis-

tributions plotted in Fig. 1, the JSD values are  $7.79 \times 10^{-6}$ ,  $7.95 \times 10^{-6}$ ,  $1.28 \times 10^{-5}$ , and  $6.78 \times 10^{-6}$ , respectively, and the mean value of the JSD over all subcarriers and blocks is about  $7.01 \times 10^{-6}$ . This indicates that the derived expression for the joint PMF closely matches its simulated counterpart for various  $k$  and  $m$  values.

In Fig. 2, we show examples of the joint PMF for various  $k$  and  $m$  values when the carrier frequency of the communications system is increased to  $f_C = 2.84968$  GHz causing  $\Delta NT_S$  to take a non-integer value, which violates the assumption A.1. The JSD values for the distributions plotted in Fig. 2 are  $1.02 \times 10^{-5}$ ,  $7.62 \times 10^{-6}$ ,  $7.84 \times 10^{-6}$ , and  $1.25 \times 10^{-5}$ , respectively, and for this example, the mean value of the JSD over all subcarriers and blocks is about  $1.50 \times 10^{-4}$ . After examining multiple non-integer values for  $\Delta NT_S$ , we concluded that the theoretical PMF remains very close to the simulated one even if  $\Delta NT_S$  is non-integer, which means that the derived PMF is robust against the loss of the assumption A.1.

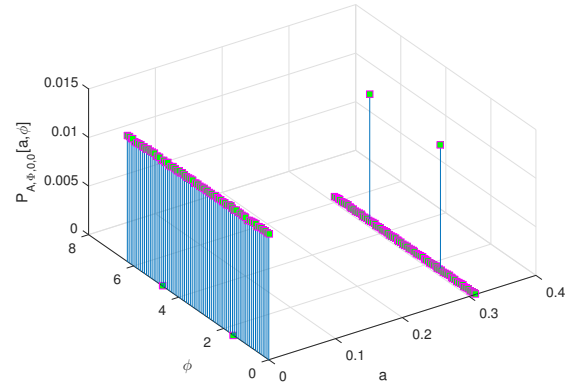
Fig. 3 considers the case of  $T_R > T_C$  (which violates the assumption A.2) and shows simulation results of the probability of having no radar interference over a specific subcarrier ( $k = 5$  in this example) as a function of the radar signal's PRI in samples,  $N_R$ . The simulation parameters used here are the same of those used in Fig. 1 with the exception of varying  $N_R$  and averaging over all blocks in the window that the communications system considers which is of length  $MN_C = 800$  samples. As expected, as  $N_R$  increases, it becomes less likely for the OFDM blocks to experience interference from a radar pulse. Moreover, the flatness in some ranges of  $N_R$  is a result of having the same number of radar pulses within the considered window for those  $N_R$  values.

An interesting case is when  $T_R$  is an integer multiple of  $T_C$ , i.e.,  $T_R = nT_C$ ,  $n \in \mathbb{Z}^+$ , wherein the interference can be seen as a cyclostationary process. Our results can be easily extended to include this case by using an indicator function of the block index,  $m$ , that is non-zero only for blocks that suffer from the interference, and for those blocks the derived PMF applies even the assumption A.2 is violated.

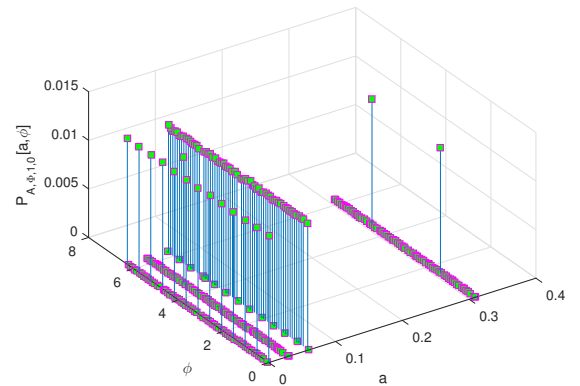
In our future work, we relax the assumption A.3 to generalize the analysis for  $T_R$ ,  $\tau_R$  and  $t_d$  values consistent with practical systems, wherein these values are not necessarily multiples of  $T_S$ , and  $\tau_R$  can be smaller than  $T_S$ . Furthermore, we consider the case in which  $t_d$  is not upper-limited by  $T_R - \tau_r$  (as in A.4) but instead, it can span multiple OFDM blocks.

## VI. CONCLUSIONS

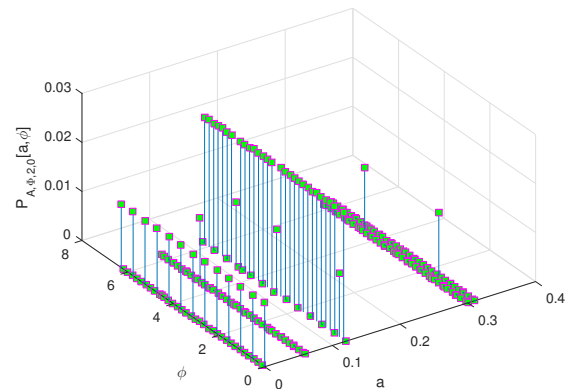
In this paper, we derived the joint PMF of the amplitude and phase of the radar interference as seen at the receiver of an OFDM-based communications system. Through simulations, we have illustrated the validity of the derived PMF for a simplified rectangular-shaped pulsed radar system. Characterizing this PMF paves the way to finding the best mechanisms of mitigating the radar interference either at the transmitter, the receiver or both. It will also help in investigating the performance and characterizing the capacity of a communi-



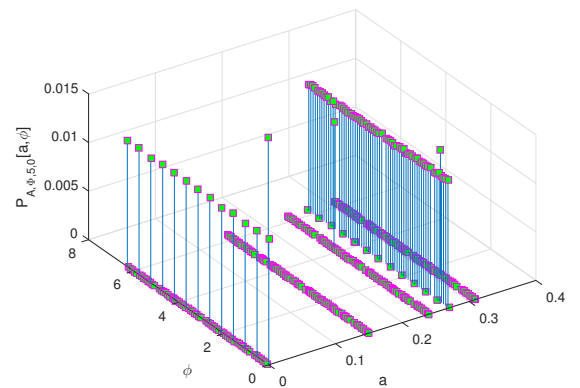
(a)  $k = 0$  and  $m = 0$ .



(b)  $k = 1$  and  $m = 0$ .

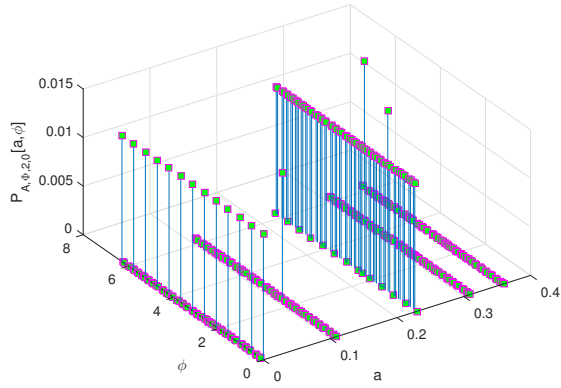


(c)  $k = 2$  and  $m = 0$ .

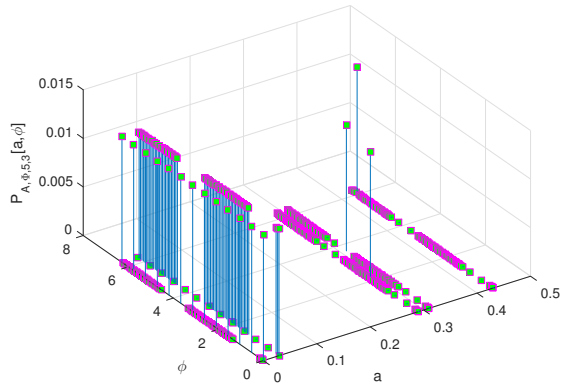


(d)  $k = 5$  and  $m = 0$ .

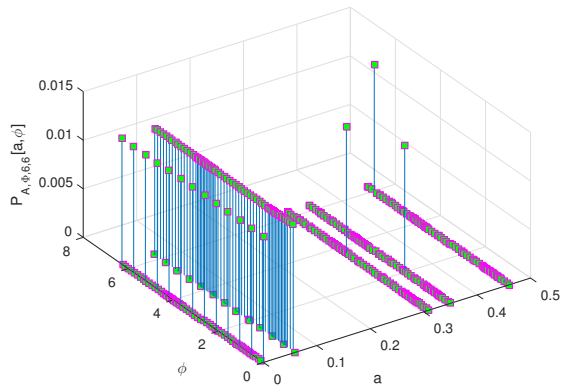
Fig. 1: Examples of the joint PMF,  $P_{A,\Phi,k,m}[a,\phi]$ , for different subcarriers during the first OFDM block.



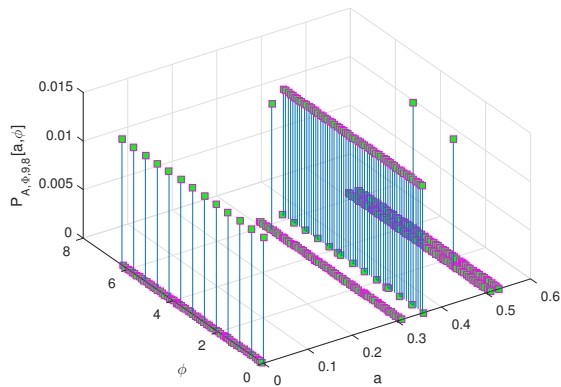
(a)  $k = 2$  and  $m = 0$ .



(b)  $k = 5$  and  $m = 3$ .



(c)  $k = 6$  and  $m = 6$ .



(d)  $k = 9$  and  $m = 8$ .

Fig. 2: Examples of  $P_{A,\Phi,k,m}[a,\phi]$  when  $\Delta NT_S$  is non-integer.

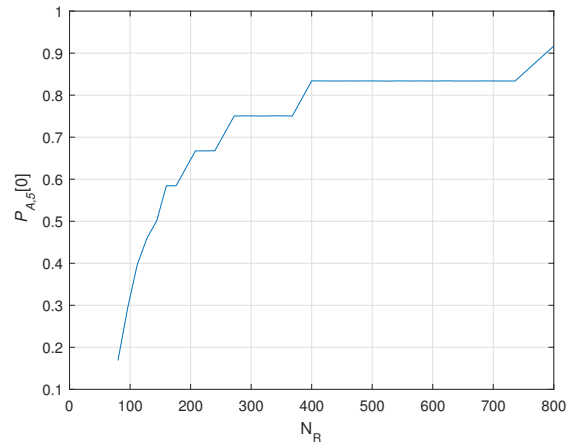


Fig. 3: Probability of having no radar interference over the 6th subcarrier versus the radar signal's PRI in samples.

cations system suffering from a radar-like interferer. As a continuation of this work, we will consider practical radar systems and model the signals used therein with abandoning the simplifying assumptions that contradict them.

#### ACKNOWLEDGMENT

The authors would like to thank Narueporn Nartasilpa for her valuable comments.

#### REFERENCES

- [1] "Enhancing access to the radio spectrum (EARS)," [http://www.nsf.gov/funding/pgm\\_summ.jsp?pims\\_id=503480](http://www.nsf.gov/funding/pgm_summ.jsp?pims_id=503480).
- [2] "Shared spectrum access for radar and communications (SSPARC)," <http://www.darpa.mil/program/shared-spectrum-access-for-radar-and-communications>.
- [3] F. H. Sanders, R. L. Sole, B. L. Bedford, D. Franc, and T. Pawlowitz, "Effects of RF interference on radar receivers," U.S. Dept. of Commerce, NTIA report TR-06-444, Sep. 2006.
- [4] L. Wang, J. McGeehan, C. Williams, and A. Doufexi, "Radar spectrum opportunities for cognitive communications transmission," in *2008 3rd International Conference on Cognitive Radio Oriented Wireless Networks and Communications (CrownCom 2008)*, May 2008, pp. 1–6.
- [5] H. Zheng, Y. Li, and Y. Zhu, "The communication solution for LTE System under radar interference circumstance," *International Journal of Antennas and Propagation*, vol. 2015, Jul. 2015.
- [6] S. Heuel and A. Roessler, "Coexistence of S-Band radar and 4g mobile networks," in *2014 15th International Radar Symposium (IRS)*, Jun. 2014, pp. 1–4.
- [7] S. Heuel, D. McCarthy, and Y. Shavit, "Test and measurement of coexistence between S-Band radar and mobile networks," in *2016 26th International Conference Radioelektronika (RA-DIOELEKTRONIKA)*, Apr. 2016, pp. 1–4.
- [8] S. Heuel, "Coexistence of S-band radar and mobile networks," [IEEE ComSoc webcast], 2016, Available: <http://host.comsoc.org/webcast/rohde3/rohde3.html>.
- [9] N. Nartasilpa, D. Tuninetti, N. Devroye, and D. Erricolo, "Let's share commrad: Effect of radar interference on an uncoded data communication system," in *2016 IEEE Radar Conference (RadarConf)*, May 2016, pp. 1–5.
- [10] N. Nartasilpa, D. Tuninetti, and N. Devroye, "On the error rate of a communication system suffering from additive radar interference," in *2016 IEEE Golbecom*, Dec 2016, pp. 1–5.
- [11] D. Tuninetti, N. Devroye, and D. Erricolo, "Characterization of the effect of radar interference on an uncoded data communication system," *IEEE Antennas and Propagation Society International Symposium/USNC-URSI National Radio Science Meeting*, Fajardo, Puerto Rico, June 26–July 1, 2016.